energies

MDPI

Article

An Innovative Methodology to Take into Account Traffic Information on WLTP Cycle for Hybrid Vehicles

Antonio Galvagno, Umberto Previti, Fabio Famoso * and Sebastian Brusca

Engineering Department, University of Messina, C. da Di Dio, 98166 Mesina, Italy; antonio.galvagno@unime.it (A.G.); umberto.previti@unime.it (U.P.); sebastian.brusca@unime.it (S.B.)
* Correspondence: ffamoso@unict.it

Abstract: The most efficient energy management strategies for hybrid vehicles are the "Optimization-Based Strategies". These strategies require a preliminary knowledge of the driving cycle, which is not easy to predict. This paper aims to combine Worldwide Harmonized Light-Duty Vehicles Test Cycle (WLTC) low section short trips with real traffic levels for vehicle energy and fuel consumption prediction. Future research can focus on implementing a new strategy for Hybrid Electric Vehicle (HEV) energy optimization, taking into account WLTC and Google Maps traffic levels. First of all, eight characteristic parameters are extracted from real speed profiles, driven in urban road sections in the city of Messina at different traffic conditions, and WLTC short trips as well. The minimum distance algorithm is used to compare the parameters and assign the three traffic levels (heavy, average, and low traffic level) to the WLTC short trips. In this way, for each route assigned from Google maps, vehicle's energy and fuel consumption are estimated using WLTC short trips remodulated with distances and traffic levels. Moreover, a vehicle numerical model was implemented and used to test the accuracy of fuel consumption and energy prediction for the proposed methodology. The results are promising since the average of the percentage errors' absolute value between the experimental driving cycles and forecast ones is 3.89% for fuel consumption, increasing to 6.80% for energy.

Keywords: HEV; WLTC; Google Maps traffic levels; driving cycles; passenger car; numerical model

Citation: Galvagno, A.; Previti, U.; Famoso, F.; Brusca, S. An Innovative Methodology to Take into Account Traffic Information on WLTP Cycle for Hybrid Vehicles. *Energies* **2021**, *14*, 1548. https://doi.org/10.3390/en14061548

Academic Editor: Hongwen He

Received: 21 February 2021
Accepted: 8 March 2021
Published: 11 March 2021

1. Introduction

One of the most Hybrid Electric Vehicle (HEV) advantages is the possibility to optimize the use of energy storage during the trip using the Energy Management System (EMS). Zhou et al. [1] categorize EMSs in:

1. Rule-Based Strategies (RBSs): These strategies define a local optimization of the powertrain's operating points. They use only the battery State of Charge (SOC) knowledge and the driver's load signal [2] to manage the vehicle's power. RBSs are easy to implement and require low computational cost, but energy management efficiency is modest. One example of RBS is presented by Bagwe et al. [3] and Wu et al. [4].
2. Optimization-Based Strategies (OBSs): These strategies define a global optimization of the powertrain's operating points. They optimize energy management by considering the car's whole Driving Cycle (DC), so the optimization depends on both internal and external parameters of the vehicle. The OBS's energy management efficiency is higher than RBS; on the other hand, they require a high computational cost, a significant complexity, and the prediction of DC. One example of OBS is presented by Fang et al. [5] and Wu et al. [6].

The scientific community is proposing numerous techniques for predicting the driving cycle. Wang et al. [7] summarize the prediction techniques in three categories:

1. Statistic and Cluster Analysis based Recognition: this category collects the techniques that use the historical and current vehicle's speed profile parameters to predict future

conditions. The techniques differ for the number of the analyzed parameters (for example, sixty-two presented by Ericson et al. [8], eleven by Xi et al. [9], and three by Chen et al. [10]), for the length of the prediction time window, and for parameter's analysis methods (Bayesian classifying algorithm, decision tree, fuzzy clustering analysis, neural network). Neural Network (NN) is the most common method according to Wang et al. [7], and it is used by Langari et al. [11], by Jeon et al. [12] and by Han et al. [13].

2. Markov Chain-Based Predictive Control: this category collects the techniques that use the current vehicle's state to predict future conditions. All the techniques are based on the stochastic Markov chain prediction process but differ for the optimization algorithm. Some examples of optimization algorithms are the Pontryagin Minimum Principle (used by Liu et al. [14]), the Stochastic Dynamic Programming (used by Johannesson et al. [15] and by Lin et al [16]), Genetic Fuzzy Logic control (used by Chaofeng et al. [17]), and NN (used by Shen et al. [18]).
3. Global Positioning System (GPS) and Intelligent Transportation Systems (ITS) based prediction: this category collects the techniques that use the historical and current vehicle's parameter, GPS, and ITS data to forecast the DC.

Numerous researches belong to the third category. Zhang et al. [19] use prior knowledge of the car's route altimetry profile (provided by GPS) to optimize the power split between energy sources in an HEV. Qiuming et al. [20] use ITS data to assign a speed profile to a specific road section. The speed profile depends on the traffic light distribution, the average speed of the vehicle's flow-rate, and the historical traffic state data. He et al. [21] use a dataset similar to Qiuming et al. [20] assigning a driving cycle in a freeway road section. The main difference is the possibility to modify the speed profile according to the car's GPS information. Zhang et al. [22] use data similar to He et al. [21], adding the near field vehicles' GPS information. A NN makes up the DC and uses it to predict each vehicle's energy expenditure for a ten-second length time window.

The third category also includes some articles that consider the Worldwide Harmonized Light-Duty Vehicles Test Cycle (WLTC). Hu et al. [23] develop an EMS optimization based on speed profile, traffic status, and road gradient knowledge. They assign to the WLTC a road grade profile and a traffic state according to a threshold velocity. It is possible to evaluate the EMS performance assuming that the vehicle under test will be in this condition. Yavasoglu et al. [24] trained a neural network to predict an electric vehicle's actual residual autonomy. The autonomy estimation is based on GPS (itinerary, road gradient profile) and ITS (traffic) information. If GPS and ITS information are not available, the neural network predicts the remaining range based on 19 training set parameters extracted from the WLTC. The NN compares the training set and the car's instantaneous parameters value to estimate the remaining autonomy.

Considering all the research, it is clear that the EMSs can forecast the vehicle's energy expenditure and fuel consumption only if many data are available. It means the use of sensor-equipped cars and cities, which is not always easy to achieve.

This paper investigates the possibility to predict the amount of fuel and energy consumed by a vehicle using a limited number of parameters and sensors to achieve a simple, easily implemented, and cost-effective prediction. The starting point of the research was the assumption that vast majority of the population and new generation vehicle can easily access GPS software (such as Google Maps). Google Maps (Mountain View, CA, USA) can provide information about the route's altitude, the distance to be driven, and the intensity of traffic. Its algorithm gives easy to read GPS and ITS data. The second assumption was that WLTC collects speed profiles made by worldwide drivers and performed in different traffic conditions, making it universal.

This paper aims to combine WLTC low section short trips with real traffic levels for vehicle energy and fuel consumption prediction.

The first step was to drive road sections in the city of Messina, recording the traffic information and speed profile provided by Google Maps (GM) and Trackaddict (HP Tuners,

Buffalo Grove, IL, USA). Only a smartphone was needed to carry out the data collection campaign, which was, therefore, extremely economical. Three databases were created containing the speed profiles collected under the same traffic condition (red in GM for high traffic intensity, yellow in GM for medium traffic intensity, and green in GM for low traffic intensity). Each database was filtered to compare the experimental speed profiles with the WLTC's short trips. Eight parameters were extracted from profiles of each database and from the individual short trips that make up the WLTC low section. Through the minimum distance calculation, parameters for each database were compared with short trips' ones. The algorithm assigned the WLTC's short trips the traffic level that best suits them. By substituting GM's road sections with the WLTC's short trips, respecting the traffic levels and distances, the DC used to forecast fuel and energy was obtained. A dynamic numerical model of a passenger car was created, using the potential of the AVL Cruise-M™ software (AVL, Graz, Austria), to evaluate the forecasting accuracy. The model setup and validation were based on literature data.

Simulations were conducted to evaluate the quality of the prediction method. The results highlight that the methodology forecasts fuel consumption and energy expenditure with acceptable errors, considering the small amount of information it requires. The GM algorithm and WLTC have worldwide nature so the study suits all cities without modifying or adding infrastructure.

2. Vehicle Mathematical Model and Validation

A dynamic numerical model was developed in the AVL Cruise-M™ environment to solve the vehicle's longitudinal motion equation. Douglas et al [25] describe a 1.6 L four-cylinder spark-ignition engine (SI) engine, Front-Wheel Drive, with a five-speed manual gearbox vehicle. This paper refers to Douglas et al. [25] for the model implementation and validation of results. Table 1 summarizes the engine specifications and the vehicle data used in the simulations.

Table 1. Vehicle and engine specifications.

Vehicle Data		
Kerb mass + 75 kg driver	1405	kg
Wheelbase	2.6	m
Front and Rear track	1.48	m
DCofG to front axle	0.95	m
HCofG to ground	0.58	m
Frontal Area	2.01	m^2
Drag Coeff	0.325	
Air Density	1.205	kg/m^3
Wheel and tire front	0.2978	m
Tire drive efficiency	0.95	
Front and rear wheel inertia	0.74	$kg{\cdot}m^2$
Gearbox Data		
Gear 1 Ratio	3.583	
Gear 2 Ratio	1.847	
Gear 3 Ratio	1.343	
Gear 4 Ratio	0.976	
Gear 5 Ratio	0.804	
Final Drive Ratio	4.052	
Engine Data		
CR	10	
Cylinders	4	
Bore	76	mm
Stroke	88	mm
Swept volume	1.5968	dm^3
Idle speed	800	rpm
Engine inertia	0.1224	$kg{\cdot}m^2$
Fuel S.G.	0.743	
Calorific Value	435,000	kJ/kg

The model calculates the thrust that the engine must provide to perform the driving cycle and to overcome the resistance's forces to motion, which are the aerodynamic drag, the rolling resistance, and the gradient loading.

Table 1 contains the data to calculate the inertia and the drag force. For the calculation of the tire rolling resistance coefficient, the method proposed by Cooper [26], expressed in Equation (1), was taken into account.

$$\begin{aligned} \mu &= 0.0085 + (0.018/p) + (1.59 \cdot 10^{-6}/p) \cdot V^2 \text{ If } V < 165 \text{ km/h} \\ \mu &= (0.018/p) + (2.91 \cdot 10^{-6}/p) \cdot V^2 \qquad \text{If } V > 165 \text{ km/h} \end{aligned} \tag{1}$$

where μ is the rolling resistance coefficient, p is the tire pressure expressed in bar and V is the vehicle velocity expressed in km/h. Douglas et al. [25] report the Engine Brake-specific fuel consumption (BSFC) map and the full load curve used to determine the vehicle's performance. The driver, modeled as PI control, generates a load signal to request traction proportional to the full load torque curve, in relation to the actual engine speed. BSFC map and the maximum torque curve of the engine are shown in Figure 1. The BSFC map numerical values are extracted by using "WebPlotPigitizer" software (Pacifica, CA, USA) and Table A1 in Appendix A shows them.

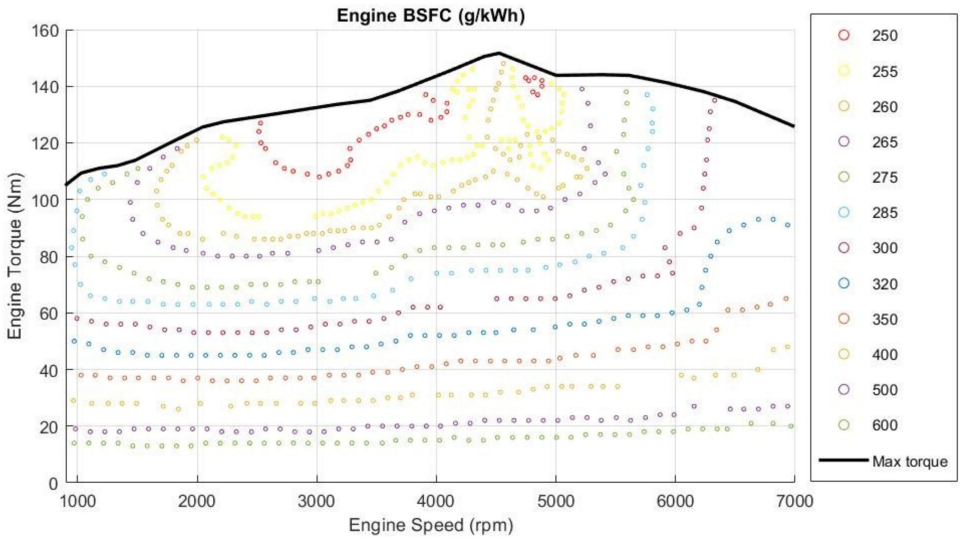

Figure 1. Engine's full load torque and Brake-specific fuel consumption (BSFC).

The map presents the full load engine's torque curve in Nm and the fuel consumption in g/kWh. Consumption was converted into g/s to implement it quickly in the AVL Cruise-M™ workspace, by the Equation (2).

$$\dot{m}_{fuel} = (BSFC \cdot N_{Eng} \cdot T_{Eng})/(3.6 \times 10^6) \tag{2}$$

where N_{Eng} is the engine's speed, T_{Eng} is the engine's torque, and BSFC represents the consumption at the operating point considered.

Figure 2 shows all the AVL Cruise-M™ library's components that build up the model and their links.

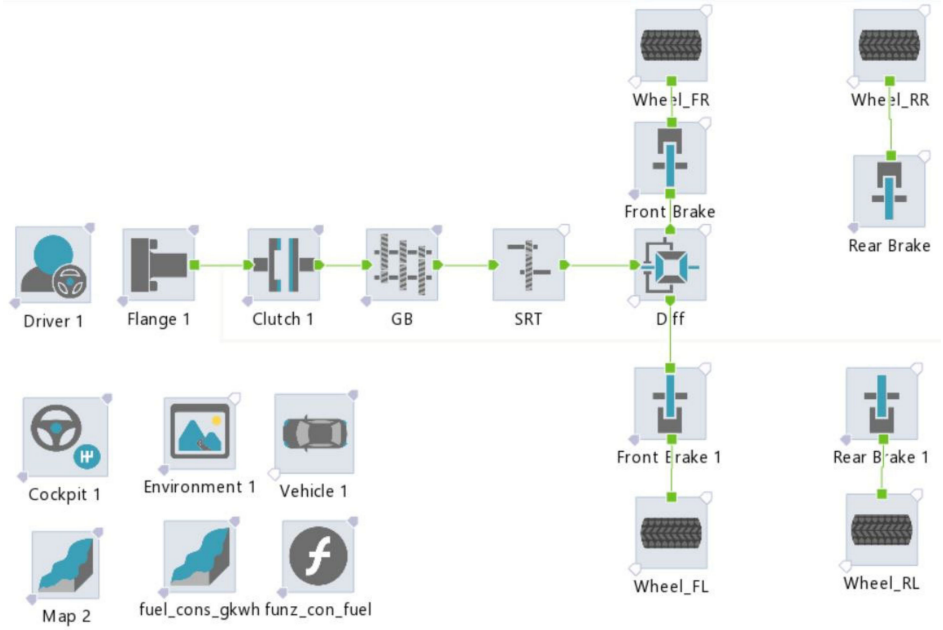

Figure 2. Vehicle's plan model on the AVL Cruise-M™ workspace.

Douglas et al. [25] present two experimental tests performed by the reference car. The first test measures the vehicle's maximum acceleration performance in 0–100 km/h speed range. The second test measures the vehicle's fuel consumption during the New European Driving Cycle (NEDC)test procedure execution. This study refers to these experimental data for numerical model validation.

2.1. Maximum Acceleration

The first simulation highlights the vehicle's performance in the acceleration from a standing start to 100 km/h. Simulation evaluates the vehicle's maximum speed too. The shifting strategy was set to perform the gear upshifting at 6700 rpm of engine speed, with a gear change duration of 0.5 s. The launching speed was set to be 1000 rpm as performed in the experimental test. For all simulation time, except during the gear change, the driver's load signal was equal to 100%. The simulated results are very similar to the experiment presented in Douglas et al. [25]. The shift from 1st to 2nd gear occurring at 4.315 s for the simulated vehicle and 4.10 s for the real one (5.24% of percentage error), the upshift from 2nd to 3rd occurs at 10.395 s, 0.2 s delay compared to the experimental data (2.92% of percentage error). Percentage error decreases at the 100 km/h (2.58%) and at the maximum velocity's evaluation (−1.01%). Figure 3 shows the correlation achieved between simulated and measured data. Table 2 collects the parameters considered for the validation of the model in this case.

Table 2. Results in maximum acceleration test.

Parameter	Simulated	Experimental	Abs Error
1st–2nd	4.315 s	4.100 s	0.215 s
2nd–3rd	10.395 s	10.100	0.295 s
0–100 km/h	11.695 s	11.400	0.295 s
Max velocity	190.05 km/h	192 km/h	1.95 km/h

From comparison with experimental data, it is possible to assert that the model describes the real vehicle with an acceptable error. Only between 0 s and 1.8 s the simulated results do not closely mimic that found in the experimental test, due probably to a different clutch release. The lack of data on clutch management makes it impossible to compare the

model and the real car in the starting phases. Inertias, efficiencies, and resistance forces of the numerical model can adequately describe the real vehicle.

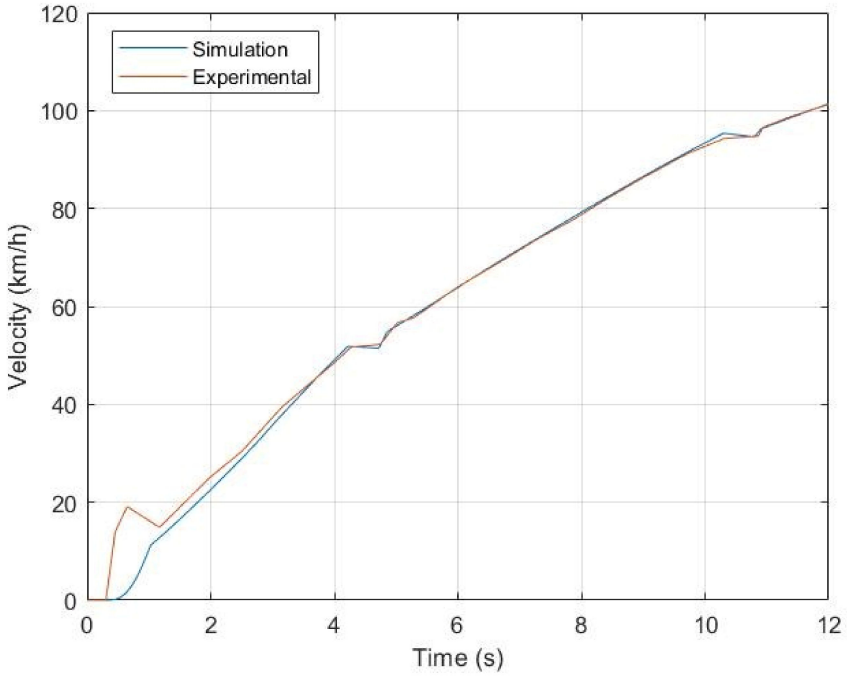

Figure 3. Maximum acceleration comparison between measured and simulated results.

2.2. NEDC Test Procedure

Following the workflow presented by Douglas et al. [25], the NEDC test procedure was simulated to validate the vehicle's fuel consumption and PI control setting. The procedure defines the gear-shifting strategy. The NEDC requires a cold start to describe the vehicle's performance adequately. Still, the Engine BSFC map was available only for steady-state operating temperature, so differences were expected from experimental tests in the "cold" region of the NEDC. To overcome this problem, Douglas et al. [25] suggest applying the corrections described in Equation (3).

$$\begin{array}{ll} \dot{m}_{\text{fuel cold}} = 4 \cdot \dot{m}_{\text{fuel hot}} & \text{If } 0 \text{ s} < t < 80 \text{ s} \\ \dot{m}_{\text{fuel cold}} = 1.4 \cdot \dot{m}_{\text{fuel hot}} & \text{If } 80 \text{ s} < t < 230 \text{ s} \end{array} \quad (3)$$

At 230 s, the engine coolant temperature is almost 85 °C, which is the engine's average running temperature. Moreover, the fuel consumption lower limit was set to 0.156 g/s to emulate the car's idle consumption. Figure 4 shows the correlation between measured and simulated fuel consumption, both instantaneous and in the accumulative form.

The fuel consumed at the end of the procedure is quite similar in both situations, with 711.00 g for the experimental data and 706.56 g for the simulation one. The percentage error is −0.62% that confirms the quality of the model. Simulated and experimental instantaneous fuel consumption are quite similar too, except for the first 230 s where the (3) is operating. Figure 5 shows the correlation between the NEDC velocity profile and vehicle velocity. PI control can manage the clutch, brake, and accelerator pedal properly.

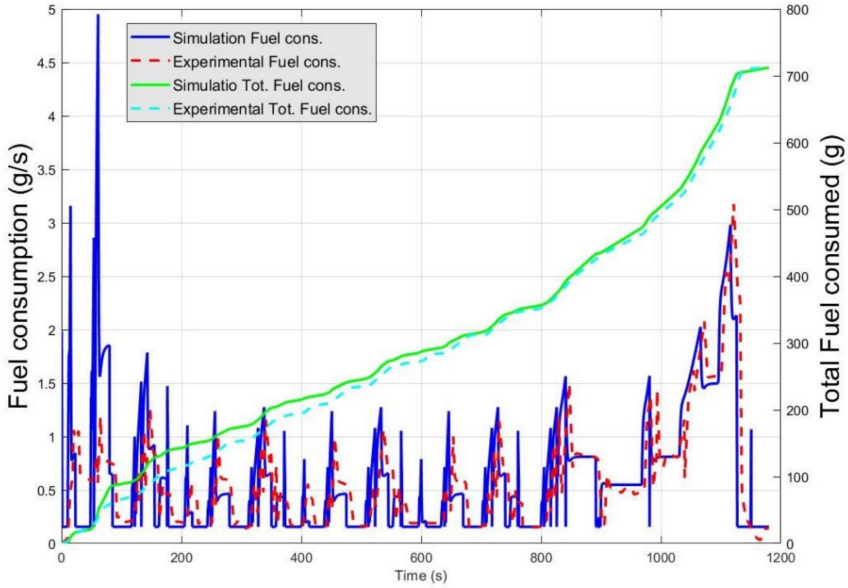

Figure 4. Fuel consumption in New European Driving Cycle (NEDC).

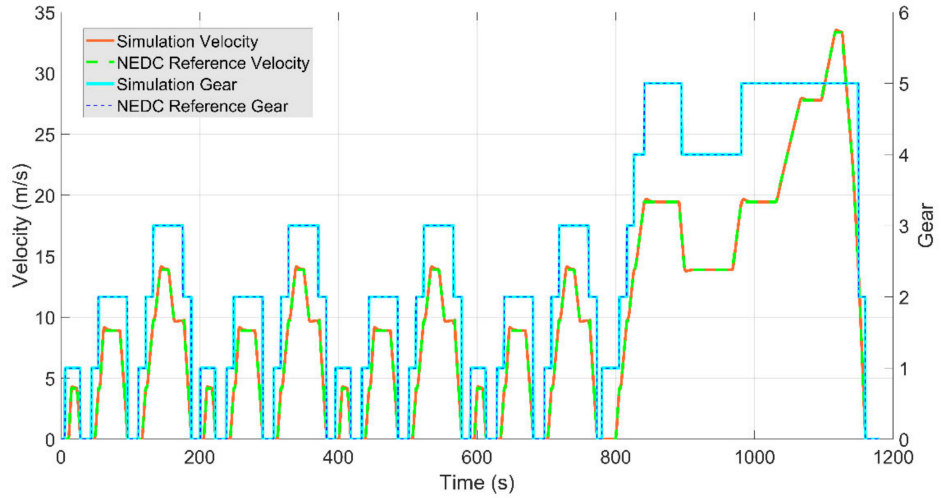

Figure 5. Speed profile and actual gear in simulation.

3. Data Collection and Processing

The same datasets presented by Previti et al. [27] were used in this study. Data collection starts with traveling road sections within the city of Messina. During the routes' execution, the TrackAddict application recorded the vehicle's speed profile while Google Maps (GM) application showed the level of service of the trip. The measurement campaign allowed the creation of three experimental DCs databases driven in three traffic conditions: High Traffic level (red in GM), Medium Traffic level (orange in GM), and Low Traffic level (green in GM).

Because the final goal is the fuel and energy forecasting comparing, through the use of WLTC, it was necessary to filter the experimental datasets following the same procedure used during the standard cycle's creation.

Tutuianu et al. [28] discuss the data filtration procedure, which consists of splitting the DCs in idling and short trips. Idle periods are the portions of the driving cycle where the speed is zero. Short trips are the portions contained between two idle periods and where the speed is non-zero, except in the first and last instants of time.

Authors continue applying elimination criteria to the short trips:

- Elimination of short trips with a duration smaller than ten seconds.
- Elimination of short trips with a maximum speed smaller than 1 m/s.
- Elimination of short trips with acceleration higher than 4 m/s^2 and smaller than -4.5 m/s^2.

After the filtering process, the databases consist of 22 short trips for the Low Traffic level database, 25 short trips for the Medium Traffic level database, and 18 short trips for the High Traffic level database. The 65 short trips represent the speed profiles in different traffic conditions in the city center of Messina. The database containing idle periods was not considered further. This paper aims to create a DC that HEVs' EMS can use to predict energy and fuel consumption. Since HEVs are equipped with start and stop systems, the power and fuel consumption during idle times are zero.

For each ST belonging to each database, the following quantities were calculated:

1. Duration.
2. Traveled distance.
3. Maximum speed.
4. Arithmetic mean of the speed.
5. Distance weighted average of speed.
6. Distance weighted average of positive acceleration.
7. Distance weighted average of negative acceleration.
8. Relative Positive Acceleration (RPA).

Equation (4) gives arithmetic mean of the speed for each short trip.

$$V_m = \sum v_{i/} n_{vi} \quad (4)$$

Being v_i the instantaneous velocity of short trip, expressed in m/s, and n_{vi} the number of measurements. Equation (5) gives the distance-weighted average of speed.

$$V_w = \sum v_i \cdot (d_i - d_{i-1}) / \sum (d_i - d_{i-1}) \quad (5)$$

The subscript i represents the time instant and d_i the distance traveled at the correspondent time instant. Distance weighted average acceleration is given by Equation (6).

$$a_w = \sum a_i \cdot (d_i - d_{i-1}) / \sum (d_i - d_{i-1}) \quad (6)$$

In which a_i represents the acceleration at the given time instant and the term $(d_i - d_{i-1})$ is the partial distance; the equation was applied to both positive and negative accelerations. Equation (7) gives the value of RPA.

$$RPA = [\int (v_i \cdot a_i^+) \cdot dt] / x \quad (7)$$

With being a_i^+ the positive acceleration and x being the total trip distance.

The eight parameters were extracted from the five short trips of the low section of the WLTC too. Only the low section was considered because experimental speed profiles were only available for urban routes.

The parameters were processed using the method of minimum distances already applied by Brusca et al. [29], in order to assign each short trip of the WLTC to a corresponding traffic level. The procedure consists of calculating the geometrical centroid for each traffic level class considering the parameters as geometrical coordinates. In this way, each short trip of the WLTC, with its corresponding parameters, was assigned to the most appropriate class by considering the shortest Euclidean distance from its centroid.

The proposed method assigned the first and the third ST of WLTC as medium traffic level, the second one as low traffic level, and the fourth and the fifth as high traffic level.

Figure 6 shows the workflow followed, from raw data to the assignment of traffic levels to the WLTC low section.

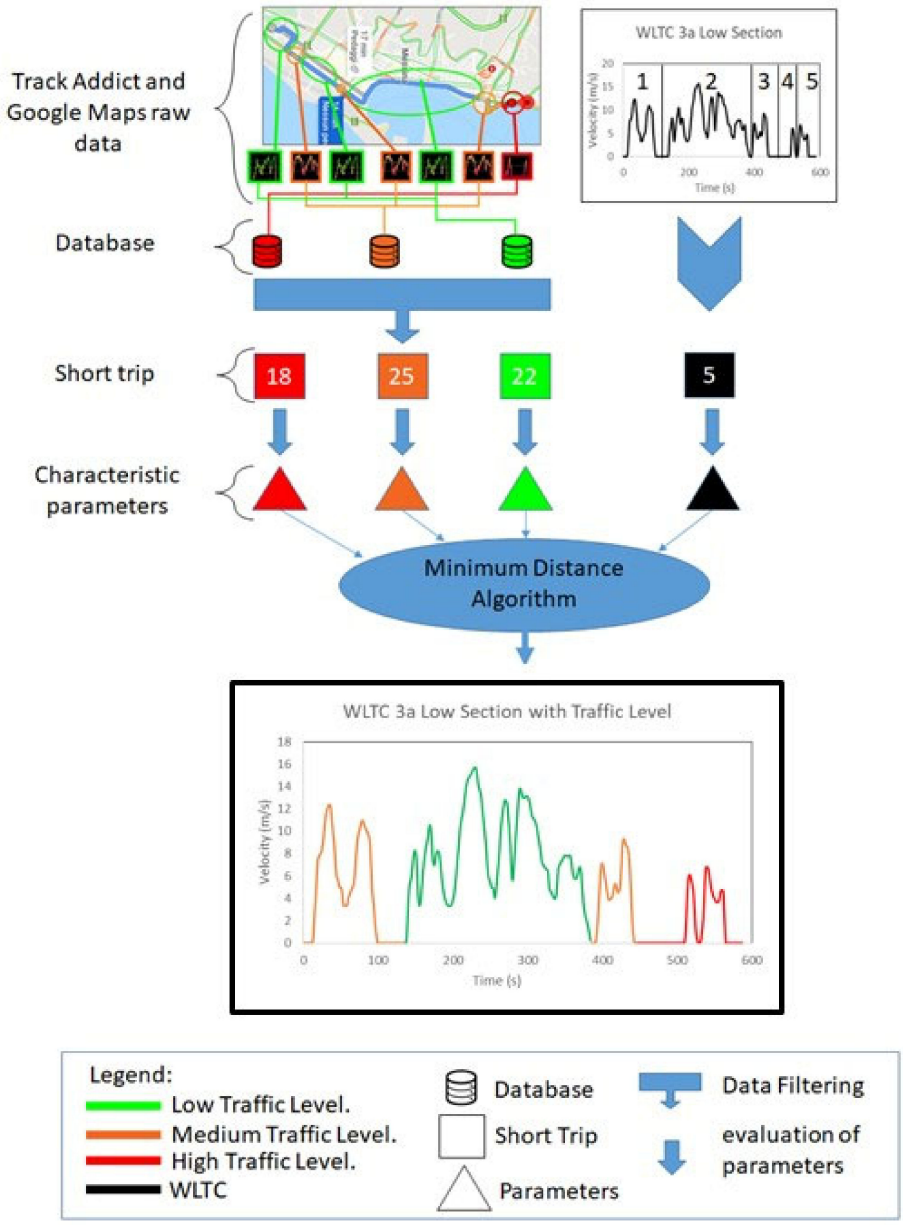

Figure 6. Data acquisition, filtering, and analysis process.

4. Simulations

Section 2 describes the numerical model used for the simulation. In the maximum acceleration validation procedure, the shifting strategy was defined by the experimental tests, while in the NEDC simulation the standard procedure provided the shift profile. A gear-change profile was not available for real driving cycles, so a shifting strategy had to be defined to conduct the simulations. The new strategy performs the gear upshifting at 3000 rpm of engine speed and the gear downshifting at 1250 rpm. The strategy allows obtaining a good range of operating points and efficiency, considering that the lowest BSFC values are between 2000 and 3000 rpm of engine speed [30]. The gear change duration remained 0.5 s, as well as the launching speed remained at 1000 rpm. The fuel consumption and energy demand were set to zero in the idling period, assuming that the car is equipped with a Start and Stop system, which is common in new-generation cars.

The forecasting method refers to Google Maps information: the distance to drive and the trip's traffic status once defining the route's starting and arrival point. The 65 short trips discussed in the previous chapter were reprocessed to replicate GM information and real

drive condition. The STs were arranged randomly, using the MatLab (Mathworks, Natick, MA, USA) function "rand", and organized into groups with ten ST. The arrangement led to the creation of six driving cycles consisting of 10 short trips and one driving cycle consisting of 5 short trips. Lastly, all the short trips, organized according to an increasing traffic level (from low to high traffic), formed the eighth driving cycle. For the eight driving cycles obtained, the distance covered and traffic level distribution were known in each time instant that is the information provided by Google Maps. The eight DCs were used to obtain the reference fuel and energy consumption value during the execution of road routes in Messina.

The knowledge of the distance to drive in different traffic conditions made it possible to construct the driving cycle to be used for fuel and energy prediction. It was sufficient to reiterate or to interrupt the WLTC short trips, respecting the assigned traffic status, until they cover the same distance as real ones.

By having the eight real driving cycles and the eight constructed ones, it was possible to calculate the real and predicted fuel consumption and energy expenditure. First, a simulation was conducted in which the driver performed the experimental cycles, evaluating the reference fuel and energy value. In the second simulation, the driver performed the driving profiles obtained from the repetition of the WLTC short trips and provided the predicted fuel and energy values. Table 3 shows the results of simulations. The first column contains the driving cycle reference number (one to eight), the second column contains the level of service distribution of each ST, and the third column shows the distance traveled in each DC. The fourth and the fifth columns contain the prediction of energy and fuel consumption accuracy, as percentage error, evaluated by Equations (8) and (9).

$$\varepsilon_{\%\ \text{energy}} = (\text{energy}_{\text{wltc}}\text{-energy}_{\text{exp}})/\text{energy}_{\text{exp}} \cdot 100 \quad (8)$$

$$\varepsilon_{\%\ \text{fuel}} = (\text{fuel}_{\text{wltc}}\text{-fuel}_{\text{exp}})/\text{fuel}_{\text{exp}} \cdot 100 \quad (9)$$

Table 3. Results. Each square is a short trip with a traffic level: red for high, orange for medium, green for low.

DC Number	Short Trips and Traffic State	Distance (m)	Energy tot. Error (%)	Fuel tot. Error (%)
1		7387	9.27	4.42
2		4317	8.75	9.33
3		9313	8.93	4.38
4		1704	1.44	−3.07
5		4077	10.39	−0.32
6		4018	10.33	1.45
7		3241	−3.00	−3.85
8 (TOT)		34,057	−2.36	−4.11

The average of the absolute values of percentage errors is 3.89% for fuel consumption, increasing to 6.80% in the energy forecast. In cycle number 8, which covers approximately 34 km, the error in energy expenditure is relatively low (−2.36%) and the fuel consumption error is similar to the average. In cycle 4, where the traveled distance is around 2 km, the prediction percentage absolute error decrease and it is lower than the average (1.44% for energy, 3.07% for fuel). The results suggest that on trips where the distance traveled at low traffic levels is predominant, the proposed methodology tends to underestimate the real values (cycles 7 and 8), but the errors remain low. In trips where distances covered at high traffic intensity are predominant, the methodology tends to overestimate the value of energy and fuel consumed.

The results are even more relevant considering that the proposed methodology:

- It only needs as input data the GM's information; no other device or software is strictly necessary. This aspect makes the methodology extremely economical.
- The algorithm regulating the traffic levels shown by GM is unique and valid in all city centers. This aspect makes the methodology universal.
- The WLTC considers the driving styles of drivers worldwide so that the methodology can be extended to any car driver.
- The prediction accuracy can increase by considering other input information, such as the traffic lights distribution or typical driver's gear shifting style. The addition of this information requires the use of appropriate infrastructure and sensors, which runs counter to the purpose of the study.

5. Conclusions

The results are promising since the average of the absolute values of percentage errors between the experimental driving cycles and forecast ones is 3.89% for fuel consumption, increasing to 6.80% for energy. The smallest percentage error in energy assessment, in absolute value, is presented in cycle number four (1.44%); for fuel assessment in cycle number five (0.32%). Cycle 5 also presented the highest percentage error in energy assessment (10.39%), while cycle 2 shows the worst fuel assessment (9.33%). The results highlight that the method can predict the considered quantities with an acceptable error (−2.36% relative percentage error for energy, −4.11% relative percentage error for fuel) in long drive city trips. The technique is easy and cheap to implement in a vehicle's EMS. The input data are universal, so they can be extended to all cities and lend themselves to the use of additional data to improve prediction accuracy. The results show a reasonable accuracy of fuel consumption and energy expenditure prediction related to the methodology detail and complexity. This study can be the basis for further studies. The possibility of predicting the energy expenditure and fuel consumption of a vehicle allows the development of energy management systems for HEVs which may:

- Manage the energy reserve to allow full electric travel to drive in Limited Traffic Zone (ZTL) or local air pollution minimization.
- Increase the life cycle of energy reserves (usually batteries) by reducing maintenance costs and disposal problems.
- Optimize the efficiency of powertrain use by reducing fuel consumption and pollutant emissions.

Author Contributions: Conceptualization, A.G. and S.B.; methodology, A.G., S.B., F.F., and U.P.; software, U.P.; writing—original draft preparation, A.G., S.B., F.F., and U.P.; writing—review and editing, A.G., S.B., F.F., and U.P.; supervision, A.G. and S.B. All authors have read and agreed to the published version of the manuscript.

Funding: This research received no external funding.

Institutional Review Board Statement: Not applicable.

Informed Consent Statement: Not applicable.

Data Availability Statement: Data sharing not applicable.

Acknowledgments: The authors are grateful to AVL Italia for providing the simulation suites, including AVL Cruise-M. They are pleased to collaborate with the company and to be able to exchange information and expertise.

Conflicts of Interest: The authors declare no conflict of interest.

Appendix A

Table A1 collects the numerical values of BSFC map used to evaluate fuel consumption.

Table A1. BSFC map numerical values function of engine speed and engine torque.

Speed (Rpm)	Torque (Nm)	BSFC (g/kWh)	Speed (Rpm)	Torque (Nm)	BSFC (g/kWh)	Speed (Rpm)	Torque (Nm)	BSFC (g/kWh)
849.0	14.3	600	3048.7	47.1	320	3503.0	85.0	265
971.2	13.8	600	3170.9	47.3	320	3620.8	86.1	265
1093.4	13.9	600	3293.1	47.6	320	3735.2	92.4	265
1215.6	13.8	600	3415.3	48.0	320	3859.6	94.8	265
1337.8	13.6	600	3537.5	48.7	320	3981.8	95.9	265
1460.0	13.4	600	3659.7	49.9	320	4104.1	96.9	265
1582.2	13.4	600	3781.9	51.6	320	4226.3	97.6	265
1704.5	13.2	600	3904.1	52.1	320	4348.5	98.3	265
1826.7	13.2	600	4026.3	51.7	320	4477.6	98.5	265
1948.8	13.4	600	4148.5	52.2	320	4599.0	98.5	265
2071.1	13.6	600	4270.7	52.5	320	4715.1	96.3	265
2193.3	13.8	600	4392.9	53.0	320	4837.3	95.6	265
2315.5	14.0	600	4498.4	53.5	320	4953.9	97.3	265
2437.7	14.4	600	4992.8	55.2	320	5075.5	99.7	265
2559.9	14.1	600	5115.0	55.9	320	5199.4	102.4	265
2682.1	14.0	600	5237.2	56.5	320	5217.2	139.4	265
2804.3	14.0	600	5359.4	57.1	320	5235.7	117.9	265
2926.5	14.2	600	5481.6	58.0	320	5266.8	133.8	265
3048.7	14.2	600	5603.8	58.6	320	5288.3	125.9	265
3170.9	14.5	600	5726.0	58.9	320	5326.1	105.9	265
3293.1	14.5	600	5848.2	59.5	320	5354.5	113.0	265
3415.3	14.4	600	5970.4	60.1	320	5411.2	109.3	265
3546.1	14.1	600	6092.6	60.9	320	2756.7	81.0	265
3659.7	14.6	600	6198.8	63.1	320	2628.9	80.6	265
3781.9	14.9	600	6219.6	68.9	320	1660.0	103.2	260
3904.1	15.2	600	6250.9	74.7	320	1665.6	98.5	260
4026.3	15.4	600	6293.8	79.9	320	1697.0	107.4	260
4148.5	15.6	600	6348.1	85.2	320	1710.0	93.3	260
4270.7	15.5	600	6448.1	89.1	320	1745.2	110.3	260
4392.9	15.5	600	6570.3	91.3	320	1760.0	90.6	260
4509.5	15.6	600	6692.5	92.8	320	1789.6	112.5	260
4637.3	15.6	600	6814.7	93.5	320	1854.4	88.5	260
4759.5	15.8	600	6936.9	91.3	320	1865.5	116.7	260
4881.7	16.0	600	7003.6	89.1	320	1915.5	119.1	260
5003.9	16.1	600	4645.6	54.0	320	1922.2	88.2	260
5126.1	16.4	600	4809.9	54.4	320	2476.5	85.7	260
5248.3	16.7	600	871.3	61.9	300	2559.9	85.8	260
5370.5	16.9	600	993.5	58.4	300	2632.1	86.0	260
5492.7	17.2	600	1115.7	57.0	300	2698.7	86.3	260
5614.9	17.2	600	1237.9	56.4	300	2770.9	86.7	260
5737.1	17.7	600	1360.1	56.0	300	2843.1	86.9	260
5859.3	17.9	600	1482.3	55.6	300	2913.1	87.7	260
5981.5	18.3	600	1604.5	54.9	300	2970.9	88.0	260
6103.7	18.7	600	1726.7	54.2	300	3046.4	88.5	260
6225.9	18.8	600	1848.9	53.6	300	3109.8	88.9	260
6348.1	19.1	600	1971.1	53.1	300	3176.4	89.0	260
6431.4	19.0	600	2093.3	52.9	300	3232.0	89.1	260
6631.4	20.9	600	2215.5	52.7	300	3387.5	89.8	260
6814.7	20.5	600	2337.7	52.7	300	3456.0	90.3	260
6964.7	20.0	600	2459.9	52.9	300	3520.8	91.4	260
860.1	19.3	500	2582.1	53.1	300	3604.1	93.8	260
982.3	19.1	500	2704.3	53.7	300	3687.5	97.4	260
1104.5	18.3	500	2826.5	54.3	300	3726.3	99.5	260
1226.7	18.0	500	2948.7	54.9	300	3820.8	102.0	260
1349.0	18.2	500	3070.9	55.5	300	3865.2	101.9	260
1471.2	18.6	500	3193.1	56.1	300	3954.1	101.1	260
1593.4	18.6	500	3315.3	56.5	300	4019.6	101.4	260

Table A1. *Cont.*

Speed (Rpm)	Torque (Nm)	BSFC (g/kWh)	Speed (Rpm)	Torque (Nm)	BSFC (g/kWh)	Speed (Rpm)	Torque (Nm)	BSFC (g/kWh)
1715.6	18.7	500	3437.5	57.2	300	4141.8	103.4	260
1837.8	18.7	500	3559.7	58.5	300	4210.7	104.7	260
1960.0	18.6	500	3681.9	60.0	300	4270.7	105.8	260
2082.2	18.6	500	3804.1	62.0	300	4326.2	107.1	260
2204.4	18.5	500	3926.3	62.1	300	4410.7	108.3	260
2326.6	18.5	500	4031.8	62.1	300	4426.2	121.8	260
2453.4	18.2	500	4504.0	64.5	300	4431.8	128.4	260
2571.0	18.7	500	4626.2	64.7	300	4454.0	131.8	260
2693.2	18.5	500	4748.4	64.7	300	4476.2	109.5	260
2815.4	18.2	500	4870.6	64.7	300	4476.2	134.8	260
2937.6	18.3	500	4992.8	65.1	300	4492.9	118.3	260
3059.8	18.3	500	5115.0	66.1	300	4498.4	138.8	260
3182.0	19.0	500	5237.2	67.6	300	4520.6	141.4	260
3304.2	19.5	500	5359.4	69.2	300	4542.9	145.1	260
3426.4	20.0	500	5481.6	70.7	300	4559.5	115.7	260
3548.6	20.2	500	5603.8	71.9	300	4559.5	147.7	260
3670.8	20.3	500	5726.0	72.8	300	4592.9	109.4	260
3793.0	20.2	500	5848.2	73.2	300	4615.1	114.0	260
3915.2	20.2	500	5910.5	82.7	300	4676.2	107.4	260
4033.7	20.2	500	5973.9	73.8	300	4692.8	115.4	260
4159.6	21.0	500	5948.2	77.8	300	4704.0	119.2	260
4281.8	21.1	500	6037.1	87.9	300	4759.5	122.7	260
4404.0	21.5	500	6153.7	89.6	300	4765.1	103.8	260
4526.2	21.9	500	6216.7	96.6	300	4837.3	101.7	260
4648.4	22.0	500	6230.7	103.7	300	4892.8	101.3	260
4770.6	22.1	500	6242.6	109.3	300	4970.6	121.4	260
4892.8	22.3	500	6267.6	120.7	300	5020.6	117.1	260
5015.0	22.0	500	6259.2	114.1	300	5020.6	103.8	260
5137.2	22.6	500	6289.5	130.6	300	5092.8	115.7	260
5259.4	22.5	500	6281.5	124.6	300	5059.4	104.6	260
5377.3	22.0	500	6325.9	134.8	300	5148.3	114.7	260
5503.8	22.5	500	965.7	88.9	285	5170.5	107.7	260
5623.5	22.5	500	949.0	82.7	285	5203.9	108.4	260
5748.2	23.3	500	976.8	76.6	285	5215.0	114.0	260
5870.4	24.1	500	1017.9	102.8	285	5259.4	110.9	260
5987.1	24.3	500	993.5	96.4	285	4855.5	122.2	260
6153.7	26.7	500	1023.1	70.1	285	3304.2	89.8	260
6457.0	25.8	500	1107.3	66.3	285	2044.9	86.5	260
6570.3	25.8	500	1109.0	107.1	285	2218.3	87.9	260
6692.5	26.3	500	1226.7	65.0	285	2327.8	87.2	260
6814.7	26.7	500	1349.0	64.4	285	1994.7	121.3	260
6936.9	27.3	500	1461.3	64.4	285	2050.4	108.2	255
7003.6	27.6	500	1586.7	64.0	285	2079.4	104.4	255
855.2	29.3	400	1715.6	62.8	285	2121.0	110.7	255
963.8	28.7	400	1837.8	62.9	285	2134.9	102.0	255
1118.1	28.5	400	1964.1	62.8	285	2187.7	111.6	255
1255.6	28.1	400	2100.2	62.9	285	2193.3	99.6	255
1371.2	28.0	400	2215.5	62.9	285	2211.0	122.0	255
1493.4	28.2	400	2337.7	62.9	285	2251.6	113.4	255
1715.0	27.4	400	2454.3	63.6	285	2268.8	97.1	255
1843.3	26.5	400	2582.1	63.4	285	2265.5	121.1	255
2026.6	27.8	400	2702.1	63.6	285	2296.9	115.5	255
2279.9	27.4	400	2825.4	63.6	285	2337.7	94.8	255
2415.4	28.2	400	2982.0	64.5	285	2326.6	118.8	255
2529.3	28.1	400	3108.4	64.5	285	2398.8	93.6	255
2659.8	27.8	400	3222.0	64.9	285	2465.4	93.8	255
2865.4	27.8	400	3326.4	65.4	285	2515.4	93.8	255
2982.0	28.2	400	3474.5	66.1	285	2987.6	94.5	255

Table A1. *Cont.*

Speed (Rpm)	Torque (Nm)	BSFC (g/kWh)	Speed (Rpm)	Torque (Nm)	BSFC (g/kWh)	Speed (Rpm)	Torque (Nm)	BSFC (g/kWh)
3116.7	29.0	400	4001.8	73.5	285	3048.7	95.0	255
3226.4	29.0	400	4126.3	74.2	285	3120.9	95.4	255
3348.6	29.3	400	4292.9	74.7	285	3187.5	96.2	255
3470.8	29.4	400	4415.1	74.7	285	3254.2	96.8	255
3593.0	29.9	400	4534.8	75.0	285	3320.8	97.6	255
3698.6	30.3	400	4659.5	75.2	285	3384.2	98.8	255
3798.5	30.7	400	4765.8	75.5	285	3454.2	100.5	255
4017.4	30.9	400	4915.0	75.9	285	3515.3	102.6	255
4124.0	30.9	400	5031.1	76.6	285	3585.6	105.8	255
4292.9	31.5	400	5159.4	78.0	285	3643.0	109.4	255
4410.7	31.0	400	5276.1	79.6	285	3698.6	112.3	255
4534.5	31.7	400	5399.7	81.4	285	3775.2	114.4	255
4687.3	32.3	400	5556.6	82.8	285	3843.0	114.6	255
4808.4	32.8	400	5648.2	87.5	285	3901.3	113.5	255
4926.1	33.6	400	5708.2	105.5	285	3976.3	112.0	255
5048.3	34.1	400	5720.4	92.7	285	4054.1	112.6	255
5131.7	34.5	400	5732.7	112.1	285	4131.8	138.8	255
5291.6	33.5	400	5742.7	98.6	285	4131.8	113.7	255
5392.7	33.9	400	5762.1	137.0	285	4175.1	141.8	255
5514.9	34.0	400	5770.4	117.6	285	4170.7	138.2	255
6048.2	38.0	400	5805.6	123.9	285	4198.5	114.5	255
6152.6	37.1	400	5809.3	131.6	285	4226.3	143.7	255
6488.8	37.6	400	5803.8	126.8	285	4239.6	128.6	255
6687.6	39.7	400	3787.8	71.9	285	4268.5	138.9	255
6818.4	47.0	400	3632.7	68.2	285	4259.6	115.4	255
6935.7	47.6	400	1223.6	109.1	285	4270.7	132.8	255
6333.8	37.9	400	1037.9	93.8	275	4274.4	121.5	255
860.1	39.3	350	1041.6	86.1	275	4298.5	146.0	255
1028.0	38.3	350	1111.5	80.2	275	4304.0	135.4	255
1146.8	37.8	350	1082.3	100.4	275	4315.1	138.6	255
1271.2	37.3	350	1171.2	103.9	275	4337.3	119.0	255
1393.4	36.9	350	1226.7	77.7	275	4309.6	116.4	255
1508.2	36.8	350	1292.2	106.5	275	4381.8	118.5	255
1637.8	36.8	350	1350.1	76.1	275	4542.9	121.0	255
1760.0	36.5	350	1413.4	109.4	275	4608.4	120.8	255
1882.2	36.5	350	1471.2	74.0	275	4604.0	118.2	255
2004.4	36.5	350	1504.5	111.3	275	4637.3	146.0	255
2126.6	36.4	350	1597.8	72.1	275	4631.7	143.3	255
2248.8	36.2	350	1715.6	70.9	275	4642.9	139.9	255
2371.0	36.4	350	1837.8	69.7	275	4659.5	120.6	255
2493.2	36.5	350	1960.0	69.1	275	4681.7	136.5	255
2612.1	36.8	350	2082.2	68.7	275	4715.1	133.2	255
2737.6	36.8	350	2204.4	68.8	275	4726.2	128.4	255
2859.8	37.1	350	2326.6	69.2	275	4765.1	125.9	255
2976.5	37.5	350	2448.8	69.6	275	4781.7	119.3	255
3104.2	37.7	350	2571.0	69.8	275	4785.4	115.5	255
3226.4	38.1	350	2697.9	70.1	275	4809.5	112.4	255
3348.6	38.4	350	2815.4	70.7	275	4842.8	124.4	255
3467.5	38.7	350	2937.6	71.1	275	4865.0	120.2	255
3593.0	39.1	350	3009.8	71.2	275	4870.6	111.3	255
3715.2	39.9	350	3493.0	74.1	275	4909.5	124.0	255
3837.4	40.7	350	3623.9	76.2	275	4903.9	115.9	255
3960.7	41.4	350	3737.4	79.7	275	4937.2	113.9	255
4081.8	42.0	350	3859.6	82.0	275	4961.7	140.7	255
4204.0	42.6	350	3980.6	82.8	275	4965.0	124.7	255
4326.2	42.7	350	4104.1	83.3	275	5026.1	138.9	255
4450.7	43.0	350	4226.3	83.4	275	5026.1	127.5	255

Table A1. *Cont.*

Speed (Rpm)	Torque (Nm)	BSFC (g/kWh)	Speed (Rpm)	Torque (Nm)	BSFC (g/kWh)	Speed (Rpm)	Torque (Nm)	BSFC (g/kWh)
4570.6	43.1	350	4348.5	83.5	275	5048.3	130.6	255
4692.8	43.1	350	4470.7	83.7	275	5053.9	133.8	255
4815.0	43.3	350	4554.0	83.9	275	5065.0	137.0	255
4937.2	43.4	350	4726.2	85.1	275	2515.4	124.0	250
5031.7	43.8	350	4848.4	85.7	275	2533.2	119.7	250
5517.7	46.5	350	4970.6	86.3	275	2571.0	117.5	250
5648.2	47.2	350	5092.8	87.1	275	3020.9	107.8	250
5770.4	47.8	350	5215.0	88.0	275	3098.7	108.9	250
5892.6	48.4	350	5337.2	89.3	275	3182.0	110.1	250
6014.8	48.9	350	5454.9	91.4	275	3256.0	111.7	250
6137.0	49.5	350	5505.7	117.0	275	3276.4	117.5	250
6253.1	50.1	350	5581.6	95.6	275	3282.0	114.4	250
6342.6	54.4	350	5570.5	128.5	275	3354.2	121.1	250
6437.0	60.5	350	5564.9	122.5	275	3431.9	123.2	250
6559.2	61.3	350	5564.9	108.9	275	3498.6	124.9	250
6681.4	61.8	350	5587.1	137.6	275	3565.3	126.1	250
6792.5	63.2	350	5592.7	134.0	275	3626.4	127.8	250
6923.0	64.7	350	5609.4	104.3	275	3699.7	129.4	250
5165.8	44.5	350	5648.2	100.4	275	3762.4	130.3	250
5311.8	45.2	350	1439.7	99.0	265	3859.6	130.2	250
849.0	52.0	320	1460.0	92.8	265	3909.6	137.0	250
971.2	49.9	320	1498.9	106.4	265	3954.1	128.2	250
1093.4	48.5	320	1545.6	87.6	265	3973.0	135.4	250
1215.6	47.4	320	1603.4	111.2	265	4037.4	129.2	250
1337.8	46.4	320	1671.1	84.9	265	4088.5	133.6	250
1460.0	45.6	320	1715.6	114.9	265	4087.4	130.8	250
1582.2	45.1	320	1797.8	83.1	265	4772.5	141.6	250
1704.4	44.7	320	1832.2	118.0	265	4806.2	138.4	250
1826.6	44.7	320	1908.1	82.1	265	4819.0	143.4	250
1948.9	44.7	320	2048.8	80.9	265	4846.1	136.9	250
2071.1	44.7	320	2171.0	80.1	265	4881.7	139.8	250
2193.3	44.7	320	2293.2	80.0	265	4881.7	142.5	250
2315.5	44.8	320	2409.9	79.9	265	2528.5	127.3	250
2437.7	45.1	320	2521.0	80.0	265	2656.3	113.5	250
2559.9	45.4	320	3015.3	82.0	265	2729.3	111.3	250
2682.1	45.7	320	3137.5	82.9	265	2802.3	110.2	250
2804.3	46.2	320	3259.7	83.8	265	2920.9	108.7	250
2926.5	46.7	320	3381.9	85.0	265	4746.0	143.4	250

References

1. Zhou, Y.; Ravey, A.; Péra, M. A survey on driving prediction techniques for predictive energy management of plug-in hybrid electric vehicles. *J. Power Sour.* **2019**, *412*, 480–495. [CrossRef]
2. Sciarretta, A.; Guzzella, L. *Vehicle Propulsion Systems: Introduction to Modeling and Optimization*, 3rd ed.; Springer: Berlin/Heidelberg, Germany, 2005.
3. Bagwe, R.M.; Byerly, A.; dos Santos, E.C., Jr.; Ben-Miled, Z. Adaptive Rule-Based Energy Management Strategy for a Parallel HEV. *Energies* **2019**, *12*, 4472. [CrossRef]
4. Wu, J.; Wei, Z.; Liu, K.; Quan, Z.; Li, Y. Battery-Involved Energy Management for Hybrid Electric Bus Based on Expert-Assistance Deep Deterministic Policy Gradient Algorithm. *IEEE Trans. Veh. Technol.* **2020**, *69*, 12786–12796. [CrossRef]
5. Fang, L.; Qin, S.; Xu, G.; Li, T.; Zhu, K. Simultaneous Optimization for Hybrid Electric Vehicle Parameters Based on Multi-Objective Genetic Algorithms. *Energies* **2011**, *4*, 532–544. [CrossRef]
6. Wu, J.; Wei, Z.; Li, W.; Wang, Y.; Li, Y.; Sauer, D. Battery Thermal- and Health-Constrained Energy Management for Hybrid Electric Bus based on Soft Actor-Critic DRL Algorithm. *IEEE Trans. Ind. Inform.* **2020**. [CrossRef]
7. Wang, R.; Lukic, S.M. Review of Driving Conditions Prediction and Driving Style Recognition Based Control Algorithms for Hybrid Electric Vehicle. In Proceedings of the 2011 IEEE Vehicle Power and Propulsion Conference, Chicago, IL, USA, 6–9 September 2011. [CrossRef]

8. Ericson, E. Independent Driving Pattern Factors and Their Influence on Fuel-Use and Exhaust Emission Factors. *Transp. Res. Part D Transp. Environ.* **2001**, *6*, 325–345. [CrossRef]
9. Xi, H.; Ying, T.; Xingui, H. An intelligent multi-feature statistical approach for discrimination of driving conditions of hybrid electric vehicle. In Proceedings of the International Joint Conference on Neural Networks, Atlanta, GA, USA, 14–19 June 2009. [CrossRef]
10. Chen, Z.; Kiliaris, L.; Murphey, Y.L.; Masrur, A. Intelligent power management in SHEV based on roadway type and traffic congestion levels. In Proceedings of the Vehicle Power and Propulsion Conference, Dearborn, MI, USA, 7–10 September 2009. [CrossRef]
11. Langari, R.; Won, J. Intelligent Energy Management Agent for a Parallel Hybrid Vehicle—Part I I: System Architecture and Design of the Driving Situation Identification Process. *IEEE Trans. Veh. Technol.* **2005**, *54*, 925–934. [CrossRef]
12. Jeon, S.; Park, Y.; Lee, J. Multi-Mode Driving Control of a Parallel Hybrid Electric Vehicle Using Driving Pattern Recognition. *J. Dyn. Sys. Meas. Control.* **2002**, *124*, 141–149. [CrossRef]
13. Han, L.; Jiao, X.; Zhang, Z. Recurrent Neural Network-Based Adaptive Energy Management Control Strategy of Plug-In Hybrid Electric Vehicles Considering Battery Aging. *Energies* **2020**, *13*, 202. [CrossRef]
14. Liu, H.; Wang, C.; Zhao, X.; Guo, C. An Adaptive-Equivalent Consumption Minimum Strategy for an Extended-Range Electric Bus Based on Target Driving Cycle Generation. *Energies* **2018**, *11*, 1805. [CrossRef]
15. Johannesson, L.; Asbogard, M.; Egardt, B. Assessing the Potential of Predictive Control for Hybrid Vehicle Powertrains Using Stochastic Dynamic Programming. *IEEE Trans. Veh. Technol.* **2007**, *8*, 71–83. [CrossRef]
16. Lin, C.; Peng, H.; Grizzle, J. Stochastic Control Strategy for Hybrid Electric Vehicles. In Proceedings of the 2004 American Control Conference, Boston, MA, USA, 30 June–2 July 2004; Volume 5, pp. 4710–4715. [CrossRef]
17. Chaofeng, P.; Wei, W.; Liao, C.; Long, C.; Limei, W. Driving range estimation for electric vehicles based on driving condition identification and forecast. *AIP Adv.* **2017**, *7*, 105206. [CrossRef]
18. Shen, P.; Zhao, Z.; Zhan, X.; Li, J.; Guo, Q. Optimal energy management strategy for a plug-in hybrid electric commercial vehicle based on velocity prediction. *Energy* **2018**, *155*, 838–852. [CrossRef]
19. Zhang, C.; Vahidi, A.; Pisu, P.; Li, X.; Tennant, K. Role of Terrain Preview in Energy Management of Hybrid Electric Vehicles. *IEEE Trans. Veh. Technol.* **2010**, *59*, 1139–1147. [CrossRef]
20. Qiuming, G.; Yaoyu, L.; Zhong-Ren, P. Optimal power management of plug-in hybrid electric vehicles. *IEEE Trans. Veh. Technol.* **2008**, *57*, 3393–3401. [CrossRef]
21. He, H.; Guo, J.; Zhou, N.; Sun, C.; Peng, J. Freeway Driving Cycle Construction Based on Real-Time Traffic Information and Global Optimal Energy Management for Plug-In Hybrid Electric Vehicles. *Energies* **2017**, *10*, 1796. [CrossRef]
22. Zhang, F.; Xi, J.; Langari, R. Real-Time Energy Management Strategy Based on Velocity Forecasts Using V2V and V2I Communications. *IEEE Trans. Veh. Technol.* **2017**, *18*, 416–430. [CrossRef]
23. Hu, J.; Jiang, X.; Jia, M.; Zheng, Y. Energy Management Strategy for the Hybrid Energy Storage System of Pure Electric Vehicle Considering Traffic Information. *Appl. Sci.* **2018**, *8*, 1266. [CrossRef]
24. Yavasoglu, Y.A.; Tetik, Y.; Gokce, K. Implementation of machine learning based real time range estimation method without destination knowledge for BEVs. *Energy* **2019**, *172*, 1179–1186. [CrossRef]
25. Douglas, K.; Milovanovic, N.; Turner, J.; Blundell, D. *Fuel Economy Improvement Using Combined CAI and Cylinder Deactivation (CDA)—An Initial Study*; SAE Technical Paper; SAE: Warrendale, PA, USA, 2005; Volume 1, p. 0110. [CrossRef]
26. Cossalter, V. *Motorcycle Dynamics*, 2nd ed.; Lulu.com: Morrisville, NC, USA, 2002.
27. Previti, U.; Brusca, S.; Galvagno, A. Passenger Car Energy Demand Assessment: A New Approach Based on Road Traffic Data. In Proceedings of the 75th National ATI Congress—#7 Clean Energy for all (ATI 2020), E3S Web Conference, Rome, Italy, 15–16 September 2020; Volume 197, p. 05006. [CrossRef]
28. Tutuianu, M.; Bonnel, P.; Ciuffo, B.; Haniu, T.; Ichikawa, N.; Marotta, A.; Pavlovic, J.; Steven, H. Development of the World-wide harmonized Light duty Test Cycle (WLTC) and a possible pathway for its introduction in the European legislation. *Trans. Res. Part D Transp. Environ.* **2015**, *40*, 61–75. [CrossRef]
29. Brusca, S.; Famoso, F.; Lanzafame, R.; Galvagno, A.; Mauro, S.; Messina, M. Wind farm power forecasting: New algorithms with simplified mathematical structure. *AIP Conf. Proc.* **2019**, *2191*, 020028. [CrossRef]
30. Oglieve, C.J.; Mohammadpour, M.; Rahnejat, H. Optimisation of the vehicle transmission and the gear-shifting strategy for the minimum fuel consumption and the minimum nitrogen oxide emissions. *Proc. Inst. Mech. Eng. Part D* **2017**, *231*, 883–899. [CrossRef]